Corrigendum

Corrigendum to "Role of climate and vegetation density in modulating denudation rates in the Himalaya" [Earth Planet. Sci. Lett. 445 (2016) 57–67]

Stephanie M. Olen *, Bodo Bookhagen, Manfred Strecker

Institute of Geosciences, University of Potsdam, 14476 Potsdam, Germany

ARTICLE INFO

Due to an error in data processing, the published denudation rates and 10-beryllium concentrations from the Sutlej valley in northwestern India are incorrect in the original article. The correct sample names, denudation rates, and ^{10}Be concentrations are included in the corrected Table 1. All statistical procedures were repeated with the corrected denudation rates. However, we note that the analysis in the original article was performed with and without the Sutlej TCN samples, due to their apparent high variability. Though a decrease in denudation variability is still observed as vegetation density increases, the apparent significance of this decrease is reduced using the corrected data. A strong positive correlation ($R = 0.89$) denudation variability with increasing vegetation seasonality is, however, still observed at statistically significant levels ($p < 0.005$). Therefore, the principle findings of the original article remain unchanged. Figs. 2, 3, 5, and 6 have been updated to reflect the corrected data (Figs. 1, 2, 3, 4).

Declaration of competing interest

The authors declare that they have no known competing financial interests or personal relationships that could have appeared to influence the work reported in this paper.

Appendix A. Supplementary material

Supplementary material related to this article can be found online at https://doi.org/10.1016/j.epsl.2020.116252.

References

Bookhagen, B., Burbank, D.W., 2010. Toward a complete Himalayan hydrological budget: spatiotemporal distribution of snowmelt and rainfall and their impact on river discharge. J. Geophys. Res., Earth Surf. 115 (F3), F03019.

Dunne, J., Elmore, D., Muzikar, P., 1999. Scaling factors for the rates of production of cosmogenic nuclides for geometric shielding and attenuation at depth on sloped surfaces. Geomorphology 27 (1–2), 3–11.

Godard, V., Bourlés, D.L., Spinabella, F., Burbank, D.W., Bookhagen, B., Fisher, G.B., Moulin, A., Léanni, L., 2014. Dominance of tectonics over climate in Himalayan denudation. Geology.

Le Roux-Mallouf, R., et al., 2015. Evidence for a wide and gently dipping Main Himalayan Thrust in western Bhutan. Geophys. Res. Lett. 42 (9), 3257–3265.

Morell, K.D., Sandiford, M., Rajendran, C., Rajendran, K., Alimanovic, A., Fink, D., Sanwal, J., 2015. Geomorphology reveals active décollement geometry in the central Himalayan seismic gap. Lithosphere 7 (3), 247–256.

Nishiizumi, K., Imamura, M., Caffee, M.W., Southon, J.R., Finkel, R.C., McAninch, J., 2007. Absolute calibration of 10Be AMS standards. Nucl. Instrum. Methods Phys. Res., Sect. B 258 (2), 403–413.

Olen, S.M., Bookhagen, B., Hoffmann, B., Sachse, D., Adhikari, D.P., Strecker, M.R., 2015. Understanding erosion rates in the Himalayan orogen: a case study from the Arun Valley. J. Geophys. Res., Earth Surf. 120 (10), 2080–2102.

Olen, S.M., Bookhagen, B., Strecker, M.R., 2016. Role of climate and vegetation density in modulating denudation rates in the Himalaya. Earth Planet. Sci. Lett. 445, 57–67.

Portenga, E.W., Bierman, P.R., Duncan, C., Corbett, L.B., Kehrwald, N.M., Rood, D.H., 2015. Erosion rates of the Bhutanese Himalaya determined using in situ - produced ^{10}Be. Geomorphology 233, 112–126.

Scherler, D., Bookhagen, B., Strecker, M.R., 2014. Tectonic control on ^{10}Be-derived erosion rates in the Garhwal Himalaya, India. J. Geophys. Res., Earth Surf. 2013JF002955.
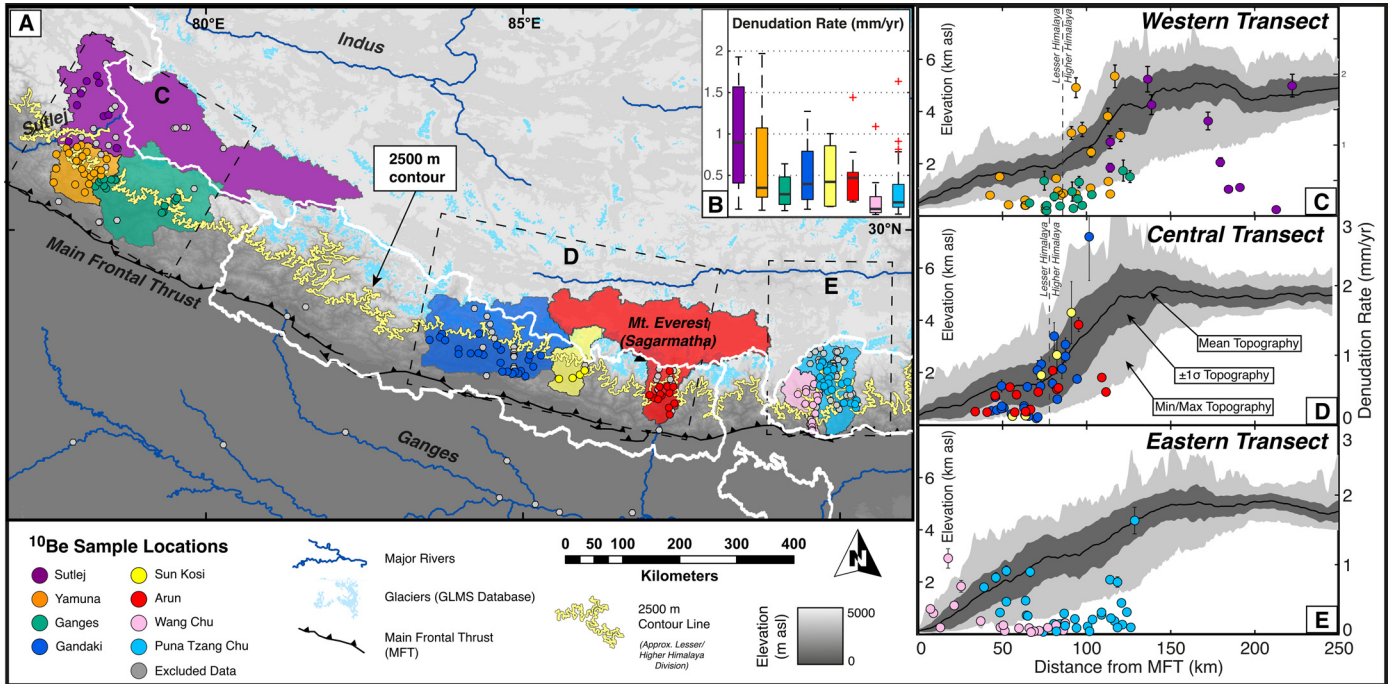
Fig. 1. Correction of Figure 2 in Olen et al. (2016). Compilation of [10]Be terrestrial cosmogenic nuclide (TCN) denudation rates from the Himalaya. (A) Digital elevation map of Himalaya (USGS GTOPO30, nominal 1-km resolution), with major rivers (dark blue), location of the Main Frontal Thrust (black), extent of present-day glaciation (light blue) (GLIMS, 2005; http://www.glims.org/), and political boundaries (white). Mt. Everest/Sagarmatha is shown for spatial reference. Sample locations (catchment centroids) of [10]Be dataset are shown as circles within major river catchments: Sutlej (purple), Yamuna (orange), Upper Ganges (green), Gandaki (dark blue), Sun Kosi (yellow), Arun (red), Wang Chu (pink), and Puna Tzang Chu (light blue). Gray circles represent samples that were excluded from the final dataset (see Supplementary Material S1–3). The approximate division of the Lesser and Higher Himalaya is shown by the 2500 m asl contour in yellow. (B) Boxplot of denudation rates from each study area from west to east, with coloring following sample color scheme in (A). Median values for each study site are represented by the thick black bar; boxes extend from the 25th to 75th percentiles; whiskers extend to all samples not considered outliers. (C–E) Strike-perpendicular swath profiles from (C) NW India (Scherler et al., 2014; Morell et al., 2015), (D) Nepal (Godard et al., 2014; Olen et al., 2015), and (E) Bhutan (Le Roux-Mallouf et al., 2015; Portenga et al., 2015). Elevation is averaged over swaths oriented perpendicular to local strike that encompass all included sample sites, denoted in (A). Thick black line denotes mean elevation, dark gray shade ±1σ, light gray shade ranges from minimum to maximum elevation values. Sample denudation rates (circles) ±1σ (vertical error bars) are plotted against the distance of the catchment centroid from the MFT, and follow the same color scheme as (A). This color scheme will be used for Figures throughout the remainder of the manuscript. (For interpretation of the references to color in this figure legend, the reader is referred to the web version of this article.)
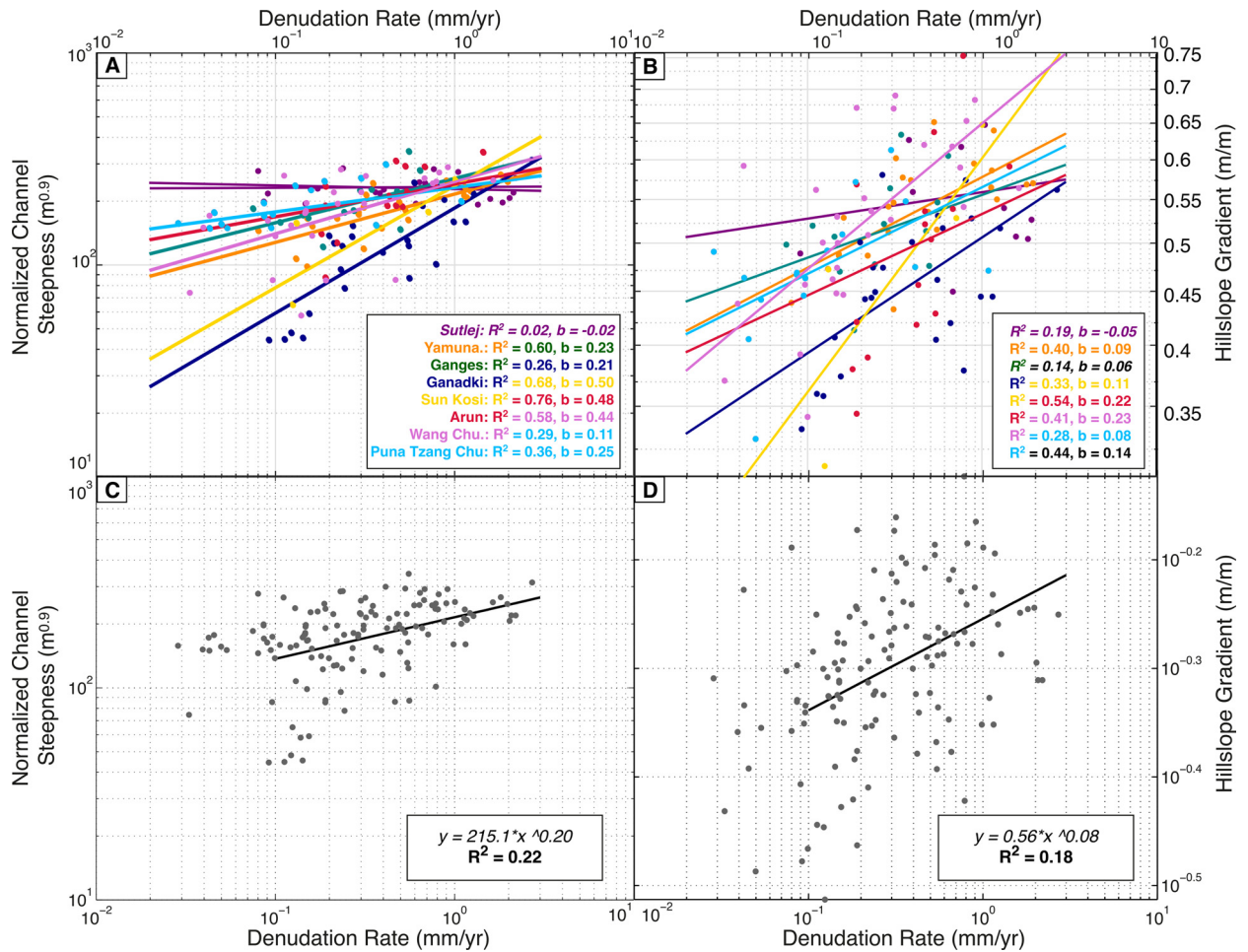
Fig. 2. Correction of Figure 3 in Olen et al. (2016). Power-law relationship between [10]Be TCN-derived denudation rates and catchment-mean values of (A, C) normalized channel steepness (ksn), and (B, D) hillslope gradient. (A) and (B) show data plotted with individual OLS power law regressions for each study area. Inset gives power law exponent b, following the relationship $f(x) = axb$, and goodness-of-fit ($R2$) for each regression. Italic text denotes where correlation is not significant at the 95% confidence level. Additional correlation statistics for each study area can be found in Table S1. (C, D) show regression for the compiled dataset, highlighting the poor fit between denudation rates and topographic metrics when all data is considered together.
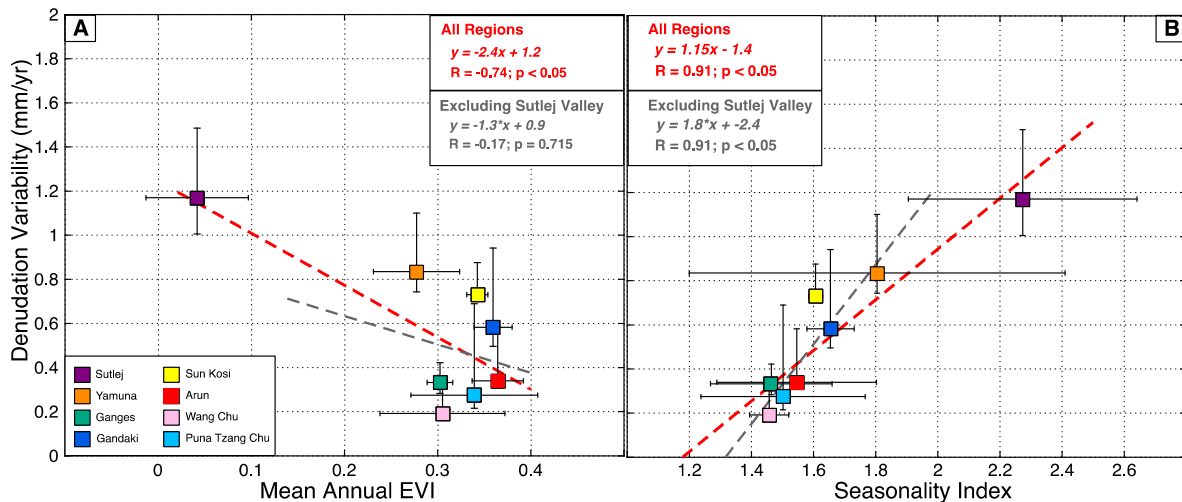
Fig. 3. Correction of Figure 5 in Olen et al. (2016). Denudation rate variability in each study area plotted against (A) mean annual EVI $\pm 1\sigma$; and (B) EVI seasonality index $\pm 1\sigma$ (summer/winter vegetation density, cf. Equation (1)). Denudation rate variability for each study area is calculated as the 75th–25th percentile of all catchment-mean denudation rates in each study area. Vertical error bars extend to the 90th–75th percentile and 25th–10th percentile. Linear OLS regressions were performed for the entire dataset (red); and for the dataset excluding the Sutlej Valley (gray). Data points are colored by major catchment, following the color scheme in Fig. 2. Correlation and regression statistics of denudation rate variability compared to all lithologic, tectonic, and climatic parameters can be found in Table S4. (For interpretation of the references to color in this figure legend, the reader is referred to the web version of this article.)
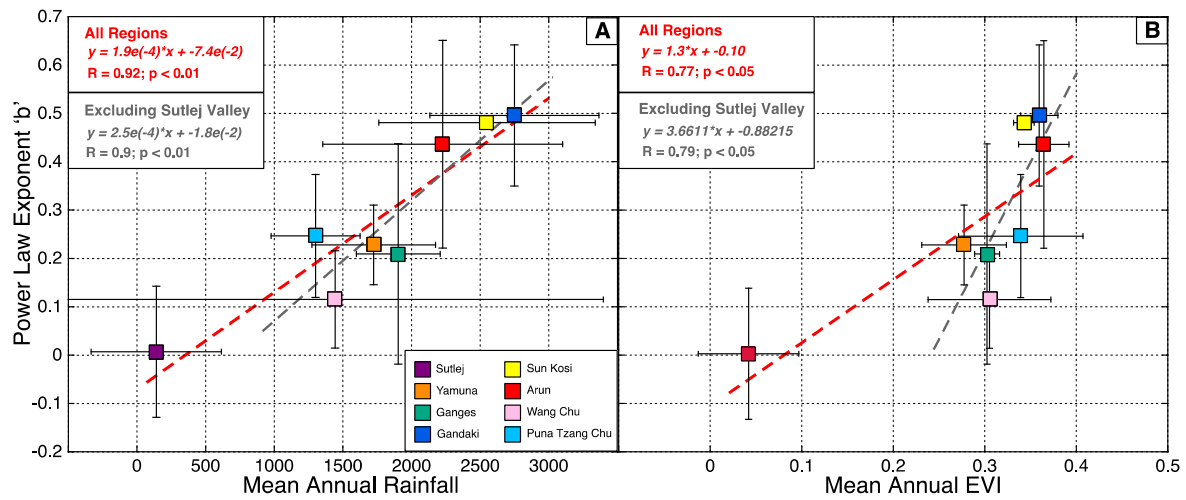
Fig. 4. Correction of Figure 6 in Olen et al. (2016). The power-law exponent *b* of the functional relationship (*topographic metric*) $\sim$ (*denudation rate*)*b* plotted against (A) mean annual rainfall $\pm 1\sigma$ and (B) mean annual EVI $\pm 1\sigma$ for each study area. Vertical error bars extend to the 95% confidence intervals of *b*. Linear OLS regressions were performed for the entire dataset (red) and for the dataset excluding the more interior Sutlej Valley (gray). Data points are colored by major catchment, following the color scheme in Fig. 2. Correlation and regression statistics of power law exponent *b* to all lithologic, tectonic, and climatic parameters can be found in Table S6. (For interpretation of the references to color in this figure legend, the reader is referred to the web version of this article.)

Table 1

Corrected Sutlej erosion rates and 10-Beryllium concentrations.

Sample Name	Sample Longitude (°)[a]	Sample Latitude (°)[a]	Denudation Rate (mm/yr)[b]	Denudation Rate Error (mm/yr)	[10]Be Conc. (atom/g)[c]	[10]Be Conc. Error (atoms/g)	Topographic Shielding[d]	Ice Shielding[e]	Snow Shielding[f]	Total Shielding
RS-1	78.18	32.10	**1.34**	**0.12**	28705.55	1408.26	0.91	1.00	0.96	0.82
RS4	78.60	31.95	**0.68**	**0.06**	71100.52	1905.97	0.95	1.00	0.98	0.88
BB18	78.19	32.12	**1.84**	**0.16**	23075.56	731.86	0.94	1.00	0.97	0.92
BB11	78.05	32.25	**0.09**	**0.01**	463186.04	8683.98	0.93	1.00	0.97	0.85
BB6	78.19	32.09	**1.34**	**0.13**	25914.38	1295.72	0.98	0.98	0.99	0.95
BB9	78.08	32.17	**0.40**	**0.03**	99565.44	1877.97	0.97	0.97	0.98	0.92
BB29	78.44	31.78	**0.38**	**0.03**	69630.77	1306.92	0.96	0.97	0.98	0.92
BB22	78.41	31.80	**0.76**	**0.06**	40502.21	838.60	0.96	0.97	0.97	0.90
B5	78.38	31.37	**1.57**	**0.14**	19440.92	767.69	0.92	0.95	0.97	0.80
N3	77.74	31.40	**1.04**	**0.09**	18070.99	564.34	0.93	0.94	0.95	0.78
RS-3	78.18	31.48	**1.93**	**0.18**	16674.31	889.38	0.90	1.00	0.99	0.90

[a] Catchment outlet coordinates.

[b] Denudation rates are calculated with a bedrock density of 2.6 g cm^{-3} and an attenuation length for spallation of $\lambda = 160$ g cm^2.

[c] Derived from blank-corrected AMS measurements undertaken at Lawrence Livermore National Laboratory and normalized to ICN standard (Nishiizumi et al., 2007).

[d] Topographic shielding based on 90-m SRTM DEM following Dunne et al. (1999).

[e] Ice shielding is based on present ice coverage from the National Snow & Ice Data Center (NSIDC) Global Land Ice Measurements from Space (GLIMS) Randolph Glacier Inventory (RGI) database (http://www.glims.org/RGI/).

[f] Snow shielding is based on model output form Bookhagen and Burbank (2010).